

Genotypic and phenotypic variation in diatom silicification under paleo-oceanographic conditions

Z. V. FINKEL,¹ K. A. MATHESON,^{1,*} K. S. REGAN^{1,†} AND A. J. IRWIN²

¹*Environmental Science Program, Mount Allison University, Sackville, NB, Canada*

²*Mathematics and Computer Science, Mount Allison University, Sackville, NB, Canada*

ABSTRACT

Diatoms have co-evolved with the silicon cycle and are largely responsible for reducing surface concentrations of silicate in the ocean to their present levels. We quantify silicification in marine diatoms at a range of high silicate concentrations representative of environments found over their geological history. The species examined include *Stephanopyxis turris*, an ancient centric species found throughout the Cenozoic, *Thalassiosira pseudonana* and *Thalassiosira weissflogii*, two younger centric species, and two pennate ecotypes of *Stauriosirella pinnata* isolated from different nutrient regimes. Frustule thickness and micromorphological structure are strongly affected by silicate concentration. All species become increasingly silicified with silicate concentrations at concentrations vastly in excess of surface ocean concentrations today. In contrast, the half-saturation constant for silicate uptake for most modern diatoms is below 2 μM . Based on the results, we hypothesize that silicate uptake is multiphasic in diatoms and that multiple silicate transport systems may have evolved in response to decreases in surface silicate concentration over geological time. The oldest species examined is more heavily silicified than the more modern species, presumably reflecting the conditions under which it originated. Yet diversification in silicification can be rapid, as illustrated by greater silicification in onshore versus the offshore ecotype of the same modern species. This work suggests that silicification of fossil frustules may eventually provide a paleoproxy for surface silicate concentrations over the Cenozoic, although development of species-specific calibrations will be necessary and the effects of a range of environmental conditions must be investigated.

Received 11 November 2009; accepted 22 May 2010

Corresponding author: Z. V. Finkel. Tel.: +1 506 364 2536; fax: +1 506 364 2583; e-mail: zfinkel@mta.ca

INTRODUCTION

Silicon is the second most abundant element in the Earth's crust. In the absence of biological activity, dissolved Si concentrations in the ocean would be in excess of 1000 μM (Siever, 1991). Currently, surface silicate concentrations range from <1 μM in the surface of much of the ocean gyres to over 100 μM in some areas of the Southern Ocean (Tréguer *et al.*, 1995). The evolution of organisms that convert dissolved Si into mineralized structures has driven a secular decrease in the availability of silicate in the surface ocean over the Phanerozoic (Maliva *et al.*, 1989; Siever, 1991; Grenne & Slack, 2003; Muttoni & Kent, 2007). Over the Paleozoic and

much of the Mesozoic, siliceous sponges and radiolarians reduced surface silicate concentrations (Siever, 1991; Racki & Cordey, 2000). The evolution and radiation of the diatoms over the Cretaceous and Cenozoic, with their ability to draw-down surface silicate to unprecedented levels, precipitated a biogeographic shift and decrease in the silicification of the spicules of siliceous sponges (Maldonado *et al.*, 1999) and tests of radiolarians (Harper & Knoll, 1975; Lazarus *et al.*, 2009). Similarly, diatom frustules may have become less silicified over time in response to decreases in silicic acid concentrations (Finkel & Kotrc, 2010). If this is the case then the silicification of fossil diatom frustules may provide a paleoproxy for surface silicate concentrations.

The oldest well-preserved diatom frustules from the Mesozoic generally appear more robust and highly silicified than more modern assemblages (Round *et al.*, 1990; Armstrong & Brasier, 2005; Finkel & Kotrc, 2010). Early Cretaceous

*Present address: Ocean Sciences Center, Memorial University, St. John's, NL, Canada

†Present address: Department of Integrative Biology, University of Guelph, Guelph, ON, Canada

diatom assemblages are dominated by centric diatoms with frustule walls that are often 1–3 μm in height, and many exhibit highly robust, highly silicified linking structures (Gersonde & Harwood, 1990; Harwood & Gersonde, 1990; Finkel & Kotrc, 2010). In contrast many modern centric and pennate species have extremely thin walls, $<<1 \mu\text{m}$, and less silicified linking structures (Finkel & Kotrc, 2010). A macro-evolutionary shift toward more lightly silicified diatom frustules is consistent with secular decreases in silicate availability over the Mesozoic and Cenozoic. Changes in diatom silicification and the length of diatom chains have probably interacted with the biogeochemistry of Si altering the residence time of silicate in the surface ocean.

Almost all diatoms have evolved an obligate requirement for silicon for growth and reproduction. In response to silicate deficiency, the cell division cycle of diatoms will be arrested at the first or second gap phases (Brzezinski *et al.*, 1990; Brzezinski, 1992; Brzezinski & Conley, 1994). Diatoms respond to silicate concentrations through the induction of a variety of silicate transporters (Thamatrakoln *et al.*, 2006; Mock *et al.*, 2008). Experimental work indicates that over current oceanic concentrations of silicate, diatom silicate uptake kinetics often follows Michaelis–Menten-type saturation kinetics (Paasche, 1973a; De La Rocha *et al.*, 2000; Martin-Jézéquel *et al.*, 2000; Leynaert *et al.*, 2009), with half-saturation coefficients that are generally $<2 \mu\text{M}$, corresponding to the surface concentrations over vast areas of the ocean (Sarmiento & Gruber, 2006).

If silicate is the only factor limiting growth, increases in silicate concentration from limiting to saturating concentrations will be associated with an increase in silicate uptake and increases in Si relative to other cellular constituents resulting in more robust frustules (Paasche, 1973b; Booth & Harrison, 1979). The degree of silicification depends on the coupling of silicate uptake relative to the assimilation of other elements associated with growth rate. For example when N, P, Fe or irradiance limits growth rate, C uptake rate decreases more than silicate uptake, resulting in an increase in Si:C (Hutchins & Bruland, 1998; Claquin *et al.*, 2002; Leynaert *et al.*, 2004; Marchetti & Harrison, 2007). As a consequence the mass of Si accumulated per unit of frustule surface area is negatively correlated with N, P, Fe and irradi-

ance limited growth rate (Hutchins & Bruland, 1998; Claquin *et al.*, 2002; Marchetti & Harrison, 2007). Much of the physiological work on the impact of silicate concentrations on diatoms has focused on growth rate and Si:C:N ratios, especially under current, often limiting, oceanic ranges of silicate concentrations. Michaelis–Menten-type uptake kinetics of silicate and increases in silicification with increasing silicate concentration suggest that Si in the frustule may increase in a predictable manner with surface water silicate concentrations and therefore might be a useful proxy for past surface silicate concentrations. Little is known about how diatom frustule morphology and silicification responds to the growth saturating surface silicate concentrations that probably characterized the ocean through the Mesozoic and much of the Cenozoic. We quantify the effect of silicate concentrations ranging from concentrations present in the current ocean under upwelling conditions to the much higher concentrations that may have been present in the Mesozoic and Cenozoic Ocean, from 20 to over 1000 μM (Siever, 1991), on diatom frustule morphology and silicification under standardized growth conditions in three centric and two pennate chain-forming diatom species isolated from a range of oceanic conditions and representing early and later frustule morphotypes.

MATERIALS AND METHODS

Experimental design and culture conditions

Diatom strains were selected to quantify the effect of high silicate concentrations on both pennate and centric diatoms isolated from a range of different environmental regimes (Table 1). All five strains were obtained from the Provasoli-Guillard National Center for the Culture of Marine Phytoplankton (CCMP): two morphologically similar marine chain-forming pennate diatom strains originally identified as *Fragilaria pinnata* now *Stausosirella pinnata* (Williams & Round, 1987; Round *et al.*, 1990), one isolated from an open ocean (CCMP 395) and the other from a coastal brackish site (CCMP 398), and three centric diatoms: *Stephanopyxis turris* (CCMP 815), *Thalassiosira pseudonana* (CCMP 1014) and *Thalassiosira weissflogii* (CCMP 1010).

Table 1 Description of experimental species. Cell volume is the average across all silicate treatments

Species	CCMP #	Cell volume (μm^3)	Habitat	Source location	Latitude ($^{\circ}\text{N}$)	Longitude ($^{\circ}\text{W}$)
<i>Stephanopyxis turris</i> (Greville et Arnott) Ralfs in Prichard	815	37 230	Coastal Ocean	Gulf of Mexico, North Atlantic	29.47	86.12
<i>Thalassiosira weissflogii</i> (Hustedt) Hasle et Heimdal	1010	1692	Open Ocean	Gulf Stream, North Atlantic	37.00	65.00
<i>Thalassiosira pseudonana</i> (Hustedt) Hasle et Heimdal	1014	40	Open Ocean	North Pacific Gyre	28.00	155.00
<i>Stausosirella pinnata</i> (Ehrhardt)	395	798	Open Ocean	Sargasso sea, North Atlantic	33.18	65.25
<i>Stausosirella pinnata</i> (Ehrhardt)	398	789	Brackish	Oyster Pond, Martha's Vinyard	41.36	70.60

The diatom cultures were grown in an artificial sea water media; all elements are added to a MilliQ (Billerica, MA, USA) filtered water source following the recipe described by Berges *et al.* (2001), except for differences in silicate concentrations. Silicon was added using appropriate amounts of a $60 \text{ g L}^{-1} \text{ Na}_2\text{SiO}_3 \cdot 9\text{H}_2\text{O}$ solution to obtain silicate concentrations of between 20 and $1100 \mu\text{M}$; all silicate concentrations are in excess of what is required for diatom species to maintain maximum growth rate. *Staurosirella pinnata* (CCMP 395, 398) were grown under 20, 50, 250, 500, $900 \mu\text{M}$ silicate, *T. pseudonana* (CCMP 1014) and *T. weissflogii* (CCMP 1010) were grown under 20, 250, $900 \mu\text{M}$ silicate and *S. turris* (815) was grown under 35, 70, 150, 550, $1100 \mu\text{M}$ silicate. Three to five separate replicate bottles were followed for each species under each silicate treatment. After a first set of experiments performed on *S. turris*, the pH of the media was set at 8.2 ± 0.1 using a 5% HCl solution. pH was checked occasionally to confirm there were no large changes over the course of the experiment. Diatom cultures were maintained in transparent polycarbonate bottles instead of glass to control silicate concentrations. All bottles were cleaned with phosphate-free detergent, soaked in 10% hydrochloric acid solution, and rinsed with Milli-Q filtered water before sterilization. Strains were maintained at 17°C and $300 \mu\text{mol quanta m}^{-2} \text{ s}^{-1}$, *S. turris* was grown under a 12:12 light–dark cycle, all other strains were exposed to continuous light.

Growth rate determination

All strains were maintained in exponential growth under each silicate treatment for a minimum of five generations in semi-continuous batch culture (Ukeles, 1973) before determining growth rate and harvesting for elemental composition and frustule morphology. Prior to the experiment, each species was grown in batch mode to determine the range in cell density during exponential growth. Throughout the experiment, cell densities were maintained below the cell densities obtained in mid-exponential phase of the batch culture thereby ensuring all cultures were optically thin and that pH and nutrient concentrations were maintained in a narrow range. Cell counts and equivalent spherical diameter were estimated using a Beckman Multisizer 3 Coulter Counter for all strains. The growth rate for each of the strains (μ, h^{-1}) was determined by linear regression of cell counts (corrected for culture dilution) over time. Counts were done in triplicate for each experimental replicate.

For the chain-forming *S. pinnata* (CCMP 395 and 398), chain length was measured using a light microscope and haemocytometer. Chain lengths were counted for all five replicates during exponential and stationary growth (3 days after the initiation of stationary phase). For all replicates, a minimum of 50 chains were counted during both exponential and stationary growth.

Elemental composition and frustule morphology

Each replicate was harvested onto 13-mm pre-combusted (5 h at 400°C) glass fiber filters for carbon and nitrogen determinations and polycarbonate filters for silica and scanning electron microscopy measurements using very low vacuum pressure, not exceeding 350 mmHg, and rinsing with a pre-filtered 3.4% NaCl solution. Two blanks were created for each set of analyses by filtering the culture media followed by the 3.4% NaCl rinse onto the appropriate filters. The polycarbonate filters were placed in Millipore filter holders using tweezers, avoiding contact with the sample, and stored in a freezer for further analysis. The glass fiber filters were folded in half, placed in a desiccator for ~ 1 week and frozen until further analysis by a CHN elemental analyzer.

Silica analysis was determined through an ammonium molybdate colorimetric assay as designed by Strickland and Parsons (1972). A 0.5% Na_2CO_3 (soda) solution was heated to 85°C (not boiling) for 2 h to extract particulate matter from the filter through hydrolysis, creating orthosilicate (Paasche, 1980). After the samples cooled, the contents were neutralized with 3.5 mL 0.5 N HCl to a pH of 3–4. The contents were transferred to a 50-mL volumetric flask and 10 mL of the ammonium molybdate reagent was added. A reducing reagent (combination of six parts 5 N sulfuric acid, 10 parts metol sulfite solution, six parts oxalic acid solution and eight parts Milli-Q H_2O) was added to the solution producing a blue color. Absorption was measured at $810 \mu\text{m}$ using a spectrophotometer. Absorption was converted to μM silicate based on a linear standard curve of absorbance for eight known concentrations of silica assayed in triplicate. Standard curves were very stable and the correlation coefficient on the linear regression was over 0.99.

Changes in frustule morphology were assayed using JEOL JSM-5600 scanning electron microscope with a 90° tilt rotary adapter. The polycarbonate filters with harvested diatom frustules were boiled in a 50:50 nitric:sulfuric acid solution for 10–30 min and rinsed several times in distilled water, lightly sonicated, and then filtered onto a new polycarbonate filter and dried. A subset of filters were examined prior to the acid treatment and showed no evidence of inorganic Si precipitation. The samples were then coated with a thin coating of gold and imaged with the scanning electron microscope. Images were taken with the sample perpendicular to the electron beam as well as at a 45° tilt angle to get estimates of the height of the frustule wall in cross-section. Under the SEM random horizontal transects were taken across the round polycarbonate filter, typically starting at the widest section of the filter. All appropriately oriented fragments along each transect were measured, until a minimum number of fragments were accumulated (usually 20–25). Preliminary investigations of the species suggest that different components of the valve are more sensitive to changes in thickness than others, and some areas are more easily accessible for measurement. For

Stephanopyxis, fragments of the mantle were measured in cross-section, for *Thalassiosira* cross-sections of fragmented valve faces were chosen, and for *S. pinnata* the length and width of the spines and cross-section of fragmented valve faces were measured.

Cell volume and surface area estimates

Cell volumes and surface area for CCMP 1014, 1010 and 815 were approximated using the thousands of measurements of the equivalent spherical diameter taken with a Coulter Counter and subsequently converted to cell diameter in valve view and cell height in girdle view using the cell diameter to height ratio (using the geometric mean) as estimated from digital images taken with a light microscope calibrated by a micrometer and assuming that these species were cylindrical. Cell volume and surface area for CCMP 395 and 398 were calculated as above except that their shape was approximated as a scalene (three unequal axes) ellipsoid. The length and width of the valve face was estimated from scanning electron micrographs and was used to calculate the height of the cell in girdle view from the Coulter Counter estimate of equivalent spherical diameter. An approximation was used to estimate the surface area of the ellipsoid = $4\pi(a^p b^p + a^p c^p + c^p b^p / 3)^{1/p}$, where a is valve length, b valve width, and c is the height of the cell in girdle view and $p = 1.6075$; this approximation yields a relative error of at most 1.061% (Thomsen, 2004).

Statistical analysis

A two-way analysis of variance (ANOVA) was used to partition the variance in Si:cell, Si:C and Si:surface area (SA) due to silicate concentration, phylogenetic (species-specific) differences in silicate usage, and the interaction between species and silicate concentration (Species \times [Si]). All five species were included and silicate concentration was treated as a linear quantitative variable. The experimental design was not completely balanced (orthogonal) and therefore the sums of squares for each of the main effects depend on the order in which they are included in the model. For this dataset, this amounted to <4% of the total variance.

RESULTS

Growth rate in response to the experimental range of silicate concentrations

Growth rate differed among strains at any given silicate treatment but did not differ significantly within any of the strains as a function of the experimental silicate treatments. The smallest diatom in this study, *T. pseudonana* CCMP 1014 has the fastest growth rate (base e) and lowest variability across silicate treatments, 0.063 ± 0.003 (h^{-1} , mean \pm standard deviation), a coefficient of variation of <5% across the silicate

treatments. The largest diatom, *S. turris* CCMP 815 has the slowest growth rate, 0.020 ± 0.002 h^{-1} , and largest variability across silicate treatments. The strains intermediate in size have intermediate growth rates across silicate treatments; *T. weissflogii* CCMP 1010 has a growth rate of 0.031 ± 0.002 h^{-1} , *S. pinnata* CCMP 395 has a growth rate of 0.032 ± 0.002 h^{-1} , and *S. pinnata* CCMP 398 has a growth rate of 0.029 ± 0.001 h^{-1} .

Changes in Si:C and Si:SA in response to increasing silicate concentrations

Si:C is lowest, 0.045 ± 0.003 mol:mol, for *S. turris* grown under 35 μM silicate, and highest, 0.88 ± 0.16 mol:mol, for *S. pinnata* CCMP 398 grown under 900 μM silicate, a ~ 20 -fold variability in Si:C. Across the silicate treatments, the largest range in Si:C was observed for the smaller species with larger surface area to volume ratios: *S. pinnata* CCMP 398 increased 14-fold, *S. pinnata* CCMP 395 increased ~ 11 -fold, and *T. pseudonana* CCMP 1014 increased over eightfold. The larger centric species examined had a more moderate increase in Si:C over the silicate treatments: *T. weissflogii* CCMP 1010 had a 3.5-fold and *S. turris* CCMP 815 had a 4.3-fold increase in Si:C. The pattern of increase in Si:C with silicate is consistent with Michaelis–Menten-type saturation kinetics with extremely high half-saturation constants for *S. turris* and *T. weissflogii* and multiphasic uptake kinetics in both strains of *S. pinnata* (Fig. 1). Due to the limited number of silicate concentrations examined, the estimates of maximum uptake velocity and the half-saturation coefficient are uncertain in several of the species examined and it is difficult to determine if the pattern in Si:C or Si:surface area with silicate concentrations is linear, saturating or multi-phasic, but there is evidence of saturation in Si:C and Si:SA in most of the strains examined at the higher silicic acid treatment. The variability in Si:C within strains across silicate treatments is generally much larger than the differences in Si:C across species at a given silicate treatment (Fig. 1). Si:cell (not shown) and Si:cell volume ratios exhibit a very similar relationships to Si:C; log cell carbon content is significantly linearly correlated with log cell volume with a slope very close to unity (slope = 1.08 with a standard error of 0.4, $r^2 = 0.9$ and sample size of 105).

Si-to-surface area ratios ($\mu\text{mol}:\mu\text{m}^2$) increase with silicate concentration for all strains up to the highest silicic acid concentrations (Fig. 1) and differ between strains at the same silicate concentration. Often species with high Si:C have lower Si:SA. The centric diatom, *S. turris* CCMP 815 which has the lowest Si:C values of the species examined has the highest values of Si:SA. *Staurosirella pinnata* CCMP 395 and 398 and *T. pseudonana* CCMP 1014 which have the highest values of Si:C have the lowest Si:SA. An anomaly in this pattern is the two *S. pinnata* strains, for both Si:C and Si:SA the open ocean strain CCMP 395 has lower values relative to the coastal strain (Fig. 1).

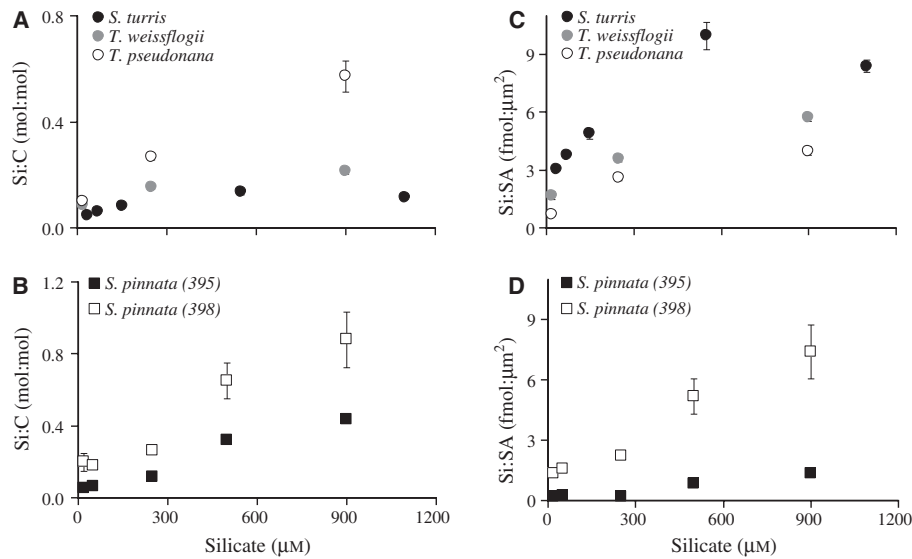


Fig. 1 Steady-state Si:C (mol:mol) \pm one standard error as a function of silicate concentration (μM) for (A) centric species and (B) pennate strains. Steady-state Si:SA (fmol: μm^2) \pm one standard error as a function of silicate concentration (μM) for (C) centric species and (D) pennate strains.

Morphological changes in the frustule in response to increasing silicate concentrations

Changes in valve morphology with silicate treatment

All species examined exhibited changes in frustule morphology with increasing silicate concentration (Figs 2 and 3, Table 2), but the degree of change and types of morphological change are species-specific.

The mantle wall of *S. turris* was much more robust, the pore size much smaller and wall height thicker in cross-section under higher silicate concentrations (Figs 2 and 3, Table 2). Thin walls are present under all silicate treatments, representing newly formed frustule walls, but an increasing number of thicker wall fragments were observed in samples exposed to increasingly high silicate concentrations, resulting in an average increase in wall thickness of 37% between the 35- and 550- μM treatments. The mantle wall was most regular and thickest under the 550- μM silicate treatment. Under 1100 μM , the wall was somewhat malformed with some infilling of the pores; this malformation may be due to lower pH levels due to the high silicate concentration (Fig. 3).

The morphological changes observed in all the other species were more subtle. In the centric species, *T. weissflogii* and *T. pseudonana*, the valve face wall thickness increased 36% and 40%, respectively, between the 20- and 900- μM treatments (Fig. 2, Table 2). The pennate, *S. pinnata* CCMP 395, exhibited a similar 36% increase in valve thickness, between the 20- and 900- μM treatment, while the valve thickness increased \sim 75% in the coastal ocean strain CCMP 398. The percentage increase in wall thickness is less than the increases

in Si:C, Si:SA and Si:cell (not shown), perhaps due to differences in the amount of silica that accumulates on different components of the frustules of different species under the different silicic acid treatments.

Linking spines and chain length

The pennate species *S. pinnata* CCMP 395 and 398 form species chains through interlocking siliceous linking spines (Fig. 2). Under exponential growth conditions silicate concentration did not have an obvious effect on average chain length in either strain but during stationary phase as nutrient availability declined (and *P* likely became limiting) and growth rate decreased, chain lengths increased for both strains under the higher silicate treatments (Fig. 4). Under exponential growth, CCMP 395 tended to be found as solitary cells or as pairs regardless of the silicate concentration. In stationary phase, chains in this strain were on average three to four cells long under 20–250 μM silicate and \sim 5 cells long under the 500- and 900- μM silicate treatments (Fig. 4). In comparison, CCMP 398 tended to form chains four to six cells long under exponential conditions regardless of silicate concentration. Under stationary conditions the chain length increased under the three highest silicate treatments, averaging \sim 11 cells per chain under 900 μM of silicate (Fig. 4). There was also a large increase in the range of chain length observed in the higher silicate treatments under stationary phase. Linking spine lengths increased an average of 32% in CCMP 398 and 50% in CCMP 395 in the 900- versus 20- μM silicate treatment. Similarly, linking spine widths increased 48% in CCMP 398 and 220% in CCMP 395 in the 900- versus 20- μM silicate treatments (Fig. 2, Table 2).

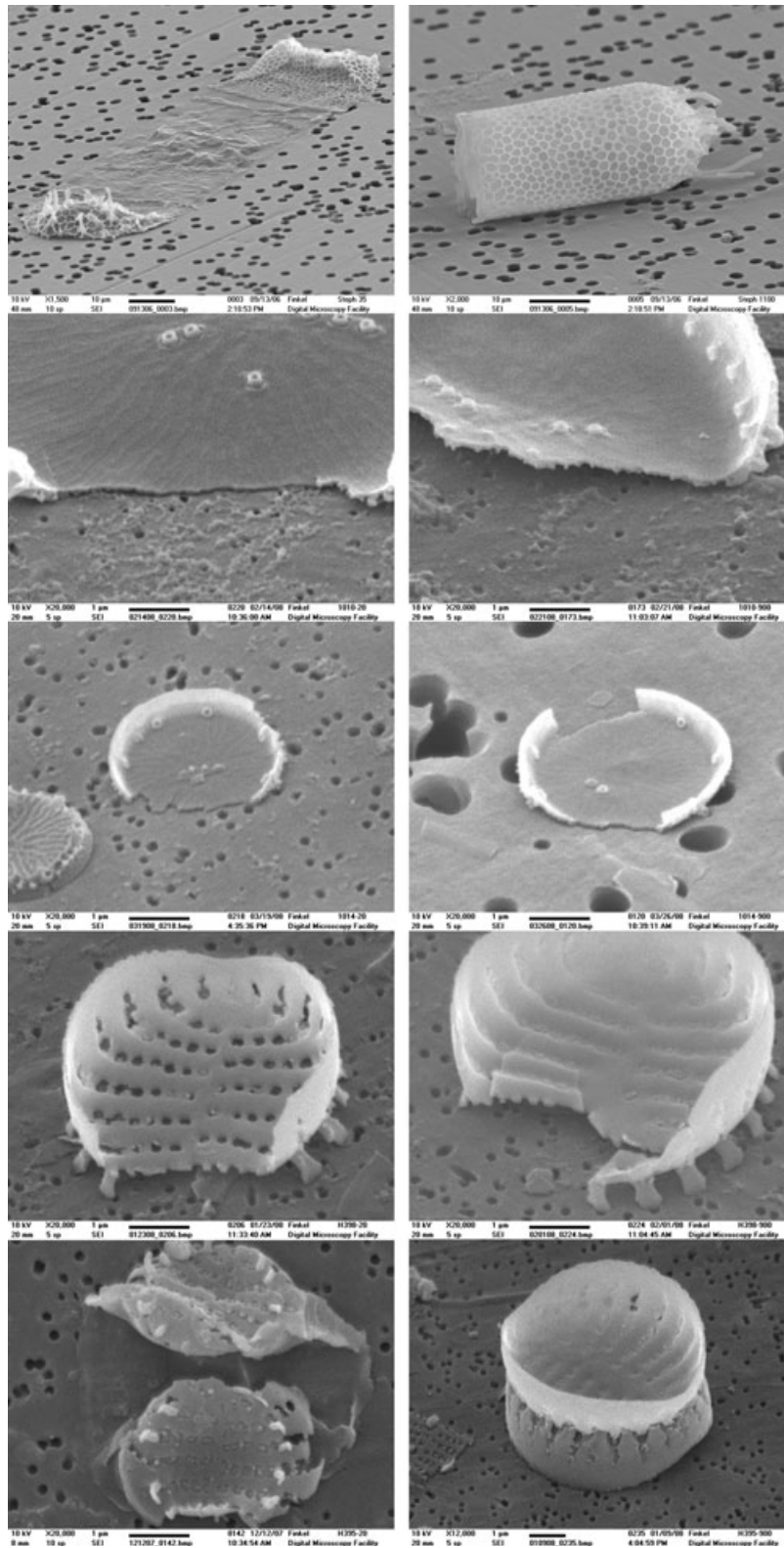


Fig. 2 Scanning electron micrographs of diatom frustules grown under low (left column) and high (right column) silicate concentrations. Note that for *Stephanopyxis turris*, low silicate was 35 μm and high silicate was 1100 μm . For the rest of the species, low silicate was 20 μm and high silicate was 900 μm . First row – *S. turris*; second row – *Thalassiosira weissflogii*, third row – *Thalassiosira pseudonana*; fourth row – *Staurosirella pinnata* (CCMP 398); fifth row – *S. pinnata* (CCMP 395).

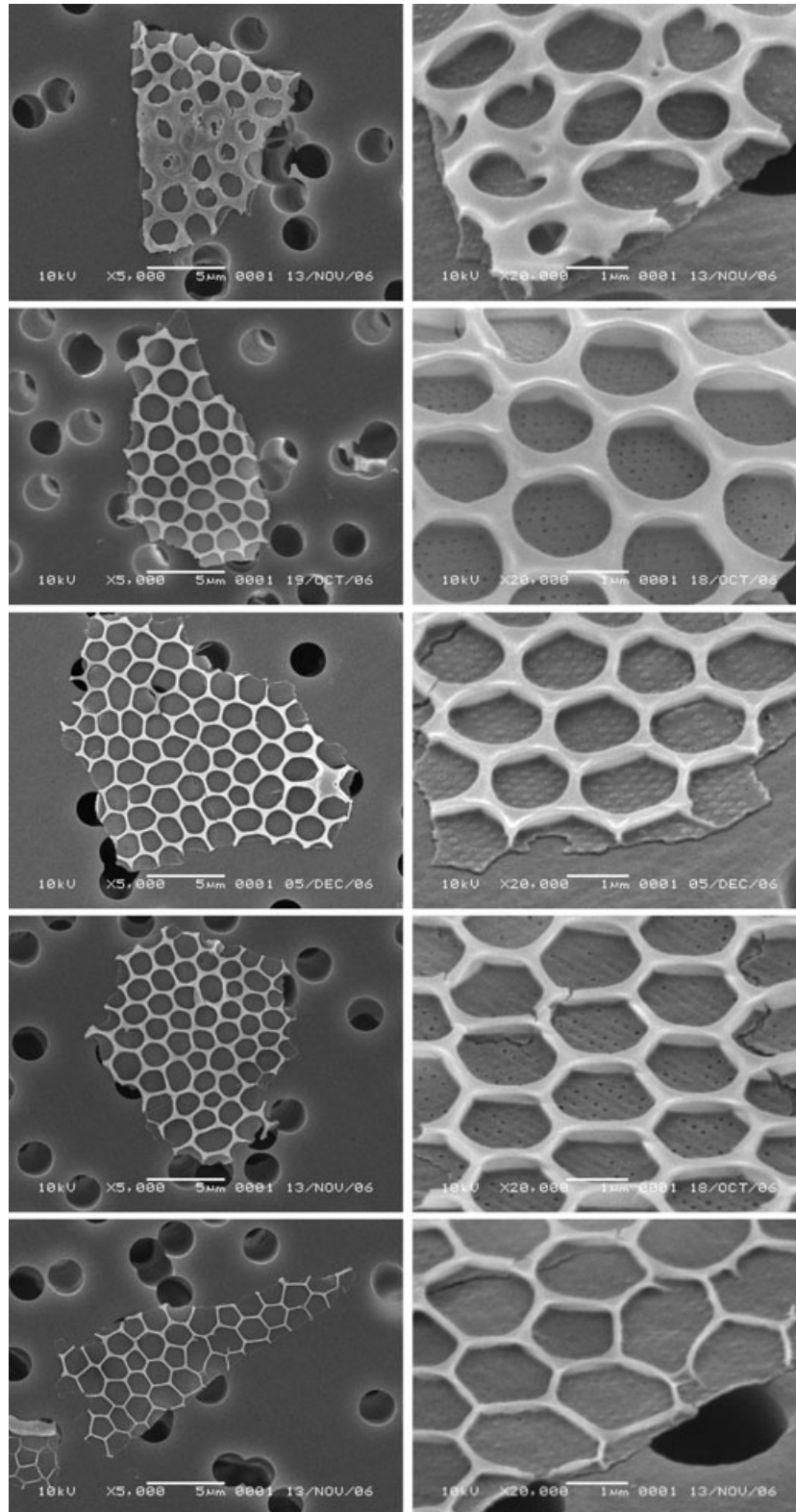
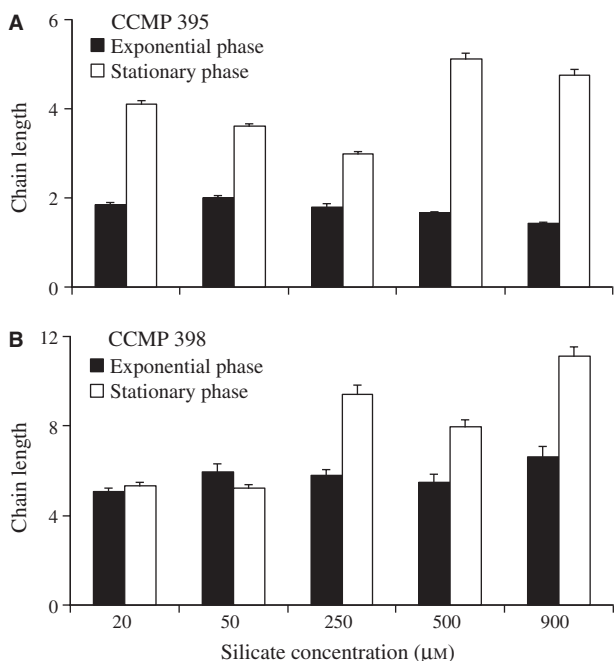


Fig. 3 Scanning electron micrographs of the micro-morphostructure of the mantle wall of *Stephanopyxis turris* grown under different silicate concentrations. First column is a top view of the frustule and the second column is at a 45° angle. Each row is a different silicate treatment decreasing from the top: 1100, 550, 250, 70, 35 μm .

Table 2 Frustule wall thickness and spine dimensions across species under low and high silicate concentrations. Sample size (*n*) refers to the number of frustule wall fragments measured in cross-section

Species	CCMP #	Low [Si]*			High [Si]*		
		Mean	SE	<i>n</i>	Mean	SE	<i>n</i>
Wall thickness (µm)							
<i>Stephanopyxis turris</i>	815	0.24	0.015	22	0.33	0.023	20
<i>Thalassiosira weissflogii</i>	1010	0.10	0.003	20	0.14	0.007	25
<i>Thalassiosira pseudonana</i>	1014	0.06	0.002	25	0.08	0.002	50
<i>Stausirella pinnata</i>	398	0.09	0.005	26	0.15	0.013	26
<i>Stausirella pinnata</i>	395	0.08	0.006	16	0.12	0.014	9
Spine length (µm)							
<i>Stausirella pinnata</i>	398	0.70	0.034	17	0.92	0.052	13
<i>Stausirella pinnata</i>	395	0.54	0.027	9	0.80	0.03	17
Spine width (µm)							
<i>Stausirella pinnata</i>	398	0.40	0.034	17	0.58	0.054	13
<i>Stausirella pinnata</i>	395	0.24	0.026	9	0.52	0.033	17

*Note that for *S. turris* low silicate is 35 µm and high silicate is 550 µm. For all other species, low silicate refers to 20 µm and high silicate refers to 900 µm.

**Fig. 4** Change in chain length (\pm one standard error) in (A) *Staurosirella pinnata* (CCMP 395) and (B) *S. pinnata* (CCMP 398), as a function of silicate concentration under exponential and stationary growth conditions.

Analysis of variance

Phenotypic response to silicate treatment, species identity, and the interaction between silicate concentration and species identity all significantly affect Si:C and Si:SA (Table 3A,B). Silicate concentration alone explains 39–31% of the variance in Si:C and Si:SA, respectively. Species identity explains an additional 27–47% of the variance in Si:C or Si:SA, respectively (Table 3). Inclusion of an interaction term between species and their response to silicate concentration increases

Table 3 (A) Analysis of variance of Si:C (mol:mol) and (B) Si:SA ($\mu\text{mol}:\mu\text{m}^2$) as a function of genotype (species) and phenotypic response to silicate concentration

(A)						
	d.f.	SS	%SS	MSS	F-value	P-value
(A) Genotypic effect (species)	4	1.20	26.9	0.30	41.5	$<10^{-16}$
(B) Phenotypic response to [Si]	1	1.75	39.2	1.75	242	$<10^{-16}$
A \times B	4	0.89	20.0	0.22	31	$<10^{-16}$
Residuals	86	0.62	13.9	0.007		
Total	95	4.47				
(B)						
	d.f.	SS ($\times 10^{-16}$)	%SS	MSS ($\times 10^{-16}$)	F-value	P-value
(A) Genotypic effect (species)	4	3.22	47.3	0.81	69.8	$<10^{-16}$
(B) Phenotypic response to [Si]	1	2.12	31.2	2.12	183.9	$<10^{-16}$
A \times B	4	0.47	6.9	0.12	10.2	$<10^{-6}$
Residuals	86	0.99	14.6	0.012		
Total	95	6.81				

the percent of total variance described to 86% for Si:C and 85% for Si:SA. These results indicate that variability in the thickness of diatom frustule walls or Si:C of diatom particulate matter reflects the species making up the assemblage and silicate concentrations they were exposed to when they deposited their frustule.

DISCUSSION

The Si cycle is regulated by and regulates the biogeographic distribution, primary and export production of diatoms (Nelson *et al.*, 1995; Tréguer *et al.*, 1995; Ragueneau *et al.*, 2000). Fossil evidence suggests that the siliceous frustules of

diatoms may have become less silicified over the Mesozoic and Cenozoic in response to their increasing success and consequent decrease in dissolved silicic acid concentrations in the ocean surface (Finkel & Kotrc, 2010). Macroevolutionary changes in the degree of silicification in diatom frustules over geological time could be due to a phenotypic response to the decreases in silicate concentrations and/or species turnover and associated evolutionary changes in the genes that control silicification. To determine if macroevolutionary decreases in the degree of silicification of diatom frustules could be due to long-term shifts in silicic acid concentrations or evolution of new silicification pathways, we quantified the effect of silicate concentrations on silicification in extant diatom species isolated from a range of oceanic conditions and representing early and later diatom frustule morphotypes. If all extant species are adapted to their more recent environmental conditions, the genes and biochemical pathways controlling silicification and response of Si:C, Si:SA and frustule thickness should be similar for older and younger morphotypes isolated from similar environmental regimes, but may differ between diatom species isolated from environments characterized by different silicic acid concentrations. In contrast, if individual extant diatom species retain a biochemical memory of the conditions under which they originated (Henderiks and Rickaby, 2007) there may be differences in the degree of silicification in response to silicic acid concentration, especially at high concentrations, between species that originated in different periods of Earth history that were characterized by higher average silicic acid concentrations.

The five diatom species examined had a significant phenotypic response in silicification in response to silicate concentrations, significant taxonomic differences in silicification at any given silicate concentration, and a significant interaction between species identity and the degree of silicification under each silicic acid concentration (Table 3). These results indicate that: (i) individual diatom species do retain genetic differences in the biochemical pathways associated with silicification and therefore may contain a biochemical memory of past environmental conditions and ii) both a phenotypic response to higher silicic acid concentrations in the geological past and species-specific changes in the transport mechanisms associated with silicification may be responsible for macroevolutionary decreases in the degree of silicification in diatom frustules since the Cretaceous.

Some of the differences in the degree of silicification between species at the same silicate concentration can be attributed to differences in cell size and the surface area to volume ratio (SA:V). The smallest species, *T. pseudonana* and the two pennate species, have the largest SA:V ratios and highest Si:C over most of the silicate concentrations examined, but not all the variability in Si:C and Si:SA is due to cell size or SA:V. Silicate uptake occurs at the cell surface and assuming the silicate uptake system is similar across the species examined, then Si:SA should be similar across species at any

particular silicate concentration under growth saturating concentrations. In fact, the different species have radically different Si:SA under similar silicate concentrations (Fig. 1, Table 3), indicating that there are significant genetic differences in silicate uptake or exudation systems between species. The species-specific differences in silicification between the older and younger diatom species are consistent with the maintenance of relic genes from ancient high-silicate environments.

Stephanopyxis turris, a species with a fossil record extending throughout the Cenozoic, has a frustule similar to many of the dominant Mesozoic diatoms, and the highest Si:SA and thickest frustule wall observed in this study, although differences in growth conditions (12:12 photo-period vs. continuous light and a lower growth rate) could be responsible for some of this difference. Diatom frustules from the Early Cretaceous tend to be heavily silicified with thick three-layered pseudoloculate cell walls that can be $\geq 1 \mu\text{m}$ thick (Finkel & Kotrc, 2010). Over the Cenozoic, there has been an increase in the diversity of thinner-walled centrics and pennate diatoms, often with smaller areolae (Finkel & Kotrc, 2010), such as the centrics *T. pseudonana* and *T. weissflogii* and the pennate strains of *S. pinnata*. Frustule wall thickness and Si:SA are comparable for the younger species *T. pseudonana*, *T. weissflogii* and *S. pinnata* CCMP 398 over much of the range of silicate concentrations examined, indicating that there may be some similarity in their silicate transport systems. In contrast, although there is little difference in cell size, surface area, or general frustule morphology between the two pennate species examined, the open ocean strain *S. pinnata* CCMP 395 had lower Si:C and Si:SA and thinner frustule walls and smaller siliceous linking spines relative to the coastal strain *S. pinnata* CCMP 398 regardless of the silicate concentration (Fig. 1, Table 2), consistent with recent adaptation of the silicate transport system in response to lower silicate concentrations. These results suggest that some diatom species may be genetically conservative, maintaining genes and biomineralization pathways over millions of years while other species are adapting their silicification pathways relatively rapidly in response to changes in their environment. Identification of genes and gene expression products from young and older extant diatom species under high and low silicic acid concentrations combined with a phylogenetic and molecular clock analysis would help confirm if silicate transport systems have evolved in response to decreasing silicate concentrations through geological time.

Decreasing silicate concentrations through the Cenozoic may have facilitated the selection of more lightly silicified diatoms with more flexible and lightly silicified linking structures. Chain formation in diatoms is wide-spread and affects nutrient uptake capacity, sinking properties, and susceptibility to grazing pressure (Smetacek, 1985; Pahlow *et al.*, 1997; Pasisak *et al.*, 2003; Raven & Waite, 2004). The siliceous linking spines for the pennate species examined became both

longer and wider with increasing silicate concentration (Table 2). The more heavily silicified linking spines were associated with longer chains during stationary growth phase as growth ceases and nutrient supply declines (Fig. 4). This suggests that as nutrients are drawn-down to growth-limiting concentrations, such as at the end of a bloom, under higher silicate concentrations some diatoms will form larger chains, which could result in higher sinking rates and export. Many of the diatom species documented in Mesozoic assemblages exhibit morphological features that suggest wide-spread chain formation through robust highly silicified linking structures (Gersonde & Harwood, 1990). Structures for chain formation in younger and modern assemblages are more varied including robust highly silicified linking structures as well as more lightly silicified structures and even chitinous threads (no Si). Unfortunately, it is difficult to assay changes in chain length from the fossil record but it would be useful to determine if longer diatom chain lengths are associated with higher diatom export efficiency over the Mesozoic and Cenozoic and more recent glacial–interglacial cycles.

Why do diatoms produce siliceous frustules? Most extant diatoms have an absolute requirement for Si for growth; the cell division cycle can be halted at two different transition points due to Si-limitation (Brzezinski, 1992; Brzezinski & Conley, 1994). It has been hypothesized that the frustule may reduce predation pressure, the likelihood of viral infection, may alter the incoming light field, perhaps acting as a photonic crystal or as sunshade, or act as a buffer for external carbonic anhydrase activity, and even modify the diffusion of nutrients [for a recent review, see Finkel & Kotrc (2010) and associated references]. The obvious costs of requiring a siliceous frustule include the metabolic cost of silicic acid uptake, reduced or arrested growth rate under low silicic acid concentrations, and increased sinking rates [see Smetacek (1985) and Raven & Waite (2004) for a more complete discussion]. The linking of the cell division cycle to a Si requirement puts the genes that control silicification, such as the genes regulating silicic acid uptake, under strong selection pressure, especially as silicic acid becomes increasingly scarce in surface waters. A conservative strategy in response to decreasing silicic acid concentrations would be to maintain high capacity, low efficiency uptake systems especially if there are still some high silicic acid regimes, while adopting ever more efficient uptake systems. Younger derived taxa, adapted to the more recent lower silicic acid conditions may be less likely to maintain the more ancient biomineralization pathways.

The degree of silicification, the amount of Si that accumulates on a cellular, cell carbon, volume, or surface area basis, is a result of the uncoupling between net silicate uptake and growth rate or carbon uptake (Harrison *et al.*, 1977; Claquin *et al.*, 2002). For example, net silicate uptake increases relative to carbon uptake with increasing silicate concentration when silicate controls growth rate in *T. pseudonana*, resulting in

thicker more regular frustules under higher silicate concentration (Paasche, 1973b). Similar changes in frustule morphology have been reported for *Thalassiosira eccentrica* and *Coscinodiscus radiatus* in silicate-limited chemostats (Booth & Harrison, 1979). Decreases in carbon fixation due to growth-limiting levels of light, nitrogen, phosphorus (Claquin *et al.*, 2002) and iron (Hutchins & Bruland, 1998; Leynaert *et al.*, 2004; Marchetti & Harrison, 2007), with relatively little change in silicate uptake, will also cause an increase in the degree of silicification. Although growth limitation by factors other than silicate concentration will tend to cause an increase Si:C (Leblanc *et al.*, 2005), laboratory work indicates that relatively small changes in silicic acid concentration have a larger quantitative impact on Si:C. For example, a slightly larger than order of magnitude decrease in free iron availability causes a 17–87% increase in Si:C in a range of *Pseudo-nitzschia* spp. (Marchetti & Harrison, 2007), while less than half an order of magnitude increase in silicate concentration results in a 250–700% increase in Si:C, in the range of species examined in this study (Fig. 1). This indicates that an order of magnitude shift in silicic acid concentrations over the Mesozoic could dominate over other factors that impact silicification.

Silicate uptake in diatoms is often described as following Michaelis–Menten-type saturation kinetics, although sigmoidal and more complex functions have been reported (Paasche, 1973a,b; Harrison *et al.*, 1976; Leynaert *et al.*, 2009). Half-saturation constants for silicate uptake as low as 0.2 μM and as high as 97 μM (for *Phaeodactylum tricornerutum*, a diatom that does not require Si to grow (Nelson *et al.*, 1984)), have been reported (Martin-Jézéquel *et al.*, 2000). Most of the diatom species examined have a half-saturation constant for silicate uptake of $<2 \mu\text{M}$ (Martin-Jézéquel *et al.*, 2000) indicating that for most species silicate uptake rate will be saturated well below 10 μM . Instead we find a hyperbolic pattern in Si:cell (not shown), Si:C, Si:SA over the concentration range of 20–1100 μM with the onset of saturation not occurring until $\sim 500 \mu\text{M}$ silicate for all three of the centric diatom species examined including *Thalassiosira pseudonana*, a species known to have a half-saturation constant of 0.8–1.5 μM for silicate uptake when grown under lower silicate concentrations. If silicate uptake follows Michaelis–Menten kinetics and the half-saturation constant is $<<20 \mu\text{M}$, and growth rate and cell size are independent of silicate concentration, as it is in this study, then increases in silicate concentrations above 20 μM should not have had any effect on silicification. For the two pennate species examined, Si:C and Si:SA appear to increase in a sigmoidal pattern; there is little change in Si:C and Si:SA from 20 to 250 and 550 to 900 μM relative to the increase from 250 to 550 μM (Fig. 1), indicative of bi- or multiphasic uptake of silicate. Recently, multiphasic uptake of silicate was documented for a benthic diatom assemblage; silicate uptake rate was hyperbolic between 0 and 60 μM but then increased linearly between 60

and 300 μM (Leynaert *et al.*, 2009). Diffusion has been invoked to explain linear increases in silicate uptake under high concentrations of substrate (Lomas & Glibert, 1999; Wischmeyer *et al.*, 2003; Leynaert *et al.*, 2009). The deviations from linearity in the increase in silicification over 250–1100 μM suggest that active transport mechanisms may be involved. We hypothesize that both benthic and planktonic diatoms have bi- or multi-phasic silicate uptake kinetics corresponding to different silicate transport systems operating over different silicate concentrations, accounting for the multiple and diverse silicate transporter genes identified from single species (Thamatrakoln *et al.*, 2006). To test this hypothesis, silicic uptake experiments should be conducted over a large range of silicic acid concentrations (from <1 to in excess of 500 μM) and the genes associated with active silicic acid uptake assayed from a range of younger and older diatom species.

Approximately, 85% of the variability in silicification, Si:C and Si:SA, in the diatoms examined can be attributed to species identity and silicate concentration. This suggests that Si:SA or wall thickness of frustule fragments (which is correlated with Si:SA) from individual diatom species, or a weighted average of the changes in silicification of numerous individual species, might be a useful proxy for large changes in surface water silicate concentrations (Figs 1–3). Measurements of Si:SA from bulk diatom assemblages will probably provide a poor estimate of silicate concentrations due to the large variability in silicification between species under the same silicate concentrations (~50% of the total variability, Table 3). Construction of a transfer function for surface silicate concentrations from Si:SA and wall thicknesses from fossilized frustules of individual diatom species will require confirmation that these patterns exist in surface waters and can be preserved in sediment, under a range of environmental conditions. Going forward the proxy could be improved by focusing solely on the thicker, mature valves that will be most responsive to changes in silicic acid concentrations and excluding newly forming valves that are always thinner than mature valves regardless of the silicic acid concentration (Tiffany & Hernández-Becerril, 2005).

CONCLUSIONS

Previous work has established that majority of diatom species tested exhibit Michaelis–Menten-type silicate uptake kinetics with half-saturation constants $\leq 2 \mu\text{M}$ when grown under modern ranges of oceanic silicate concentrations. In this study, we show that individual diatom species become more heavily silicified with increasing silicate concentrations over the range of 20–1100 μM . The increase in Si:C and Si:SA over this extended range of silicic acid concentrations is best described as sigmoidal for the two pennate species and Michaelis–Menten-type for the three centric diatom species examined, although more silicate treatments and silicic acid uptake experiments are required to properly characterize the

kinetics of steady-state silicate uptake. We hypothesize that diatoms have bi- or multi-phasic uptake systems for silicate, with one transport system operating below and another above 20 μM silicate. Species-specific differences in Si:C and Si:SA at the same silicate concentration are parsimonious with an evolutionary change in silicate transport systems that arose in response to decreases in silicate concentration in the ocean through the Mesozoic and Cenozoic as well as variations in surface silicate availability in the ocean. The strong relationship between individual species' Si:SA and diatom frustule thickness with silicate concentration over a large range of silicate concentrations suggests that a weighted average of changes in the frustules thickness of specific species may be a useful paleoproxy for surface silicate concentrations under conditions where nutrient (N, P, Fe) and light-growth limitation (Martin-Jézéquel *et al.*, 2000; Claquin *et al.*, 2002) and predator-induced (Sommer, 1998; Pondaven *et al.*, 2007) increases in silicification are secondary to this primary signal.

ACKNOWLEDGMENTS

We thank Jim Ehman and Mount Allison's Digital Microscopy facility for the SEM work. Z.V.F. was supported by NSERC, CFI and NBIF, A.J.I. was supported by NSERC, and K.M. was supported by an NSERC undergraduate award. We thank three anonymous referees for their comments.

REFERENCES

- Armstrong H, Brasier MD (2005) *Microfossils*. Wiley-Blackwell, Malden, MA.
- Berges JA, Franklin DJ, Harrison PJ (2001) Evolution of an artificial seawater medium: improvements in enriched seawater, artificial water over the past two decades. *Journal of Phycology* **37**, 1138–1145.
- Booth B, Harrison PJ (1979) Effect of silicate limitation on valve morphology in *Thalassiosira* and *Coscinodiscus* (Bacillariophyceae). *Journal of Phycology* **15**, 326–329.
- Brzezinski MA (1992) Cell-cycle effects on the kinetics of silicic acid uptake and resource competition among diatoms. *Journal of Plankton Research* **14**, 1511–1539.
- Brzezinski MA, Conley DJ (1994) Silicon deposition during the cell cycle of *Thalassiosira weissflogii* (Bacillariophyceae) determined using dual rhodamine 123 and propidium iodide staining. *Journal of Phycology* **30**, 45–55.
- Brzezinski MA, Olson RJ, Chisholm SW (1990) Silicon availability and cell-cycle progression in marine diatoms. *Marine Ecology Progress Series* **67**, 83–96.
- Claquin P, Martin-Jézéquel V, Kromkamp J, Veldhuis M, Kraay GW (2002) Uncoupling of silicon compared with carbon and nitrogen metabolisms and the role of the cell cycle in continuous cultures of *Thalassiosira pseudonana* (Bacillariophyceae) under light, nitrogen and phosphorus control. *Journal of Phycology* **38**, 922–930.
- De La Rocha CL, Hutchins DA, Brzezinski MA, Zhang YH (2000) Effects of iron and zinc deficiency on elemental composition and silica production by diatoms. *Marine Ecology-Progress Series* **195**, 71–79.

- Finkel ZV, Kotrc B (2010) Silica use through time: macroevolutionary change in the morphology of the diatom frustule. *Geomicrobiology Journal* (in press).
- Gersonde R, Harwood DM (1990) Lower Cretaceous diatoms from ODP Leg 113 Site 693 (Weddell Sea). Part I: vegetative cells. In *Proceedings of the Ocean Drilling Program Scientific Results*, Vol. 113 (eds Barker PF, Kennett JP, O'Connell S, Berkowitz S, Bryant WR, Burckle LH, Egeberg PK, Fiitterer DK, Gersonde RE, Golovchenko X, Hamilton N, Lawver L, Lazarus DB, Lonsdale M, Mohr B, Nagao T, Pereira CPQ, Pudsey CJ, Robert CM, Schandl E, Spiejb V, Stott LD, Thomas E, Thompson KFM, Wise SW Jr). Ocean Drilling Program, College Station, TX, pp. 365–402.
- Grenne T, Slack J (2003) Paleozoic and Mesozoic silica-rich seawater: evidence from hematitic chert (jasper) deposits. *Geology* **31**, 319–322.
- Harper HE Jr, Knoll AH (1975) Silica, diatoms, and Cenozoic radiolarian evolution. *Geology* **3**, 175–177.
- Harrison PJ, Conway HL, Dugdale RC (1976) Marine diatoms grown in chemostats under silicate or ammonium limitation. I. Cellular chemical composition and steady-state growth kinetics of *Skeletonema costatum*. *Marine Biology* **35**, 177–186.
- Harrison PJ, Conway HL, Holmes RW, Davis CO (1977) Marine diatoms grown in chemostats under silicate or ammonium limitation. III. Cellular chemical composition and morphology of *Chaetoceros debilis*, *Skeletonema costatum*, and *Thalassiosira gravida*. *Marine Biology* **43**, 19–31.
- Harwood DM, Gersonde R (1990) Lower Cretaceous diatoms from ODP Leg 113 Site 693 (Weddell Sea). Part 2: resting spores, chrysophycean cysts, an endoskeletal dinoflagellate, and notes on the origins of the diatoms. In *Proceedings of the Ocean Drilling Program Scientific Results*, Vol. 113 (eds Barker PF, Kennett JP, O'Connell S, Berkowitz S, Bryant WR, Burckle LH, Egeberg PK, Fiitterer DK, Gersonde RE, Golovchenko X, Hamilton N, Lawver L, Lazarus DB, Lonsdale M, Mohr B, Nagao T, Pereira CPQ, Pudsey CJ, Robert CM, Schandl E, Spiejb V, Stott LD, Thomas E, Thompson KFM, Wise SW Jr). Ocean Drilling Program, College Station, TX, pp. 403–425.
- Henderiks J, Rickaby REM (2007) A coccolithophore concept for constraining the Cenozoic carbon cycle. *Biogeosciences* **4**, 323–329.
- Hutchins DAB, Bruland K (1998) Iron-limited diatom growth and Si:N uptake ratios in a coastal upwelling regime. *Nature* **393**, 561–564.
- Lazarus DB, Kotrc B, Wulf G, Schmidt DN (2009) Radiolarians decreased silicification as an evolutionary response to reduced Cenozoic ocean silica availability. *Proceedings of the National Academy of Sciences of the USA* **106**, 9333–9338.
- Leblanc K, Hare CE, Boyd PW, Bruland KW, Sohst B, Pickmere S, Lohan MC, Buck K, Ellwood M, Hutchins DA (2005) Fe and Zn effects on the Si cycle and diatom community structure in two contrasting high and low-silicate HNLC areas. *Deep Sea Research I* **52**, 1842–1864.
- Leynaert A, Bucciarelli E, Claquin P, Dugdale R, Martin-Jézéquel V, Pondaven P, Ragueneau O (2004) Effect of iron on diatom cell size and silicic acid uptake kinetics. *Limnology and Oceanography* **49**, 1134–1143.
- Leynaert A, Longphuiet SN, Claquin P, Chauvaud L, Ragueneau O (2009) No limit: The multiphasic uptake of silicic acid by benthic diatoms. *Limnology and Oceanography* **54**, 571–576.
- Lomas MW, Glibert PM (1999) Temperature regulation of nitrate uptake: a novel hypothesis about nitrate uptake and reduction in cool-water diatoms. *Limnology and Oceanography* **44**, 556–572.
- Maldonado M, Carmona MC, Uriz MJ, Cruzado A (1999) Decline in Mesozoic reef-building sponges explained by silicon limitation. *Nature* **401**, 785–788.
- Maliva RG, Knoll AH, Siever R (1989) Secular change in chert distribution: a reflection of evolving biological participation in the silica Cycle. *Palaios* **4**, 519–532.
- Marchetti A, Harrison PJ (2007) Coupled changes in cell morphology and the elemental (C, N, and Si) composition of the pennate diatom *Pseudo-nitzschia* due to iron deficiency. *Limnology and Oceanography* **52**, 2270–2284.
- Martin-Jézéquel V, Hildebrand M, Brzezinski MA (2000) Silicon metabolism in diatoms: implications for growth. *Journal of Phycology* **36**, 821–840.
- Mock T, Samanta MP, Iverson V, Berthiaume C, Robison M, Holtermann K, Durkin C, Splinter BonDurant S, Richmond K, Rodesch M, Kallas T, Huttlin EL, Cerrina F, Sussman MR, Armbrust EV (2008) Whole-genome expression profiling of the marine diatom *Thalassiosira pseudonana* identifies genes involved in silicon bioprocesses. *Proceedings of the National Academy of Sciences of the USA* **105**, 1579–1584.
- Muttoni G, Kent DV (2007) Widespread formation of cherts during the early Eocene climate optimum. *Palaeogeography, Palaeoclimatology, Palaeoecology* **253**, 348–362.
- Nelson DM, Riedel GF, Millan-Nunez R, Lara-Lara JR (1984) Silicon uptake by algae with no known Si requirement. I. True cellular uptake and pH-induced precipitation by *Phaeodactylum tricoratum* (Bacillariophyceae) and *Platymonas* sp. (Prasinophyceae). *Journal of Phycology* **20**, 140–147.
- Nelson DM, Treguer P, Brzezinski MA, Leynaert A, Queguiner B (1995) Production and dissolution of biogenic silica in the ocean - revised global estimates, comparison with regional data and relationship to biogenic sedimentation. *Global Biogeochemical Cycles* **9**, 359–372.
- Paasche E (1973a) Silicon and the ecology of marine plankton diatoms. II. Silicate uptake kinetics in five diatoms species. *Marine Biology* **19**, 262–269.
- Paasche E (1973b) Silicon and the ecology of marine plankton diatoms. I. *Thalassiosira pseudonana* (*Cyclotella nana*) grown in a chemostat with silicate as limiting nutrient. *Marine Biology* **19**, 117–126.
- Paasche E (1980) Silicon content of five marine plankton diatom species measured with a rapid filter method. *Limnology and Oceanography* **25**, 474–480.
- Pahlow M, Riebesell U, Wolf-Gladrow DA (1997) Impact of cell shape and chain formation on nutrient acquisition by marine diatoms. *Limnology and Oceanography* **42**, 1660–1672.
- Pasikak J, Soroczki-Pinter E, Rezner Z (2003) Sinking properties of some phytoplankton shapes and the relation of form resistance to morphological diversity of plankton - an experimental study. *Hydrobiologia* **500**, 243–257.
- Pondaven P, Gallinari M, Chollet S, Bucciarelli E, Sarthou G, Schultes S, Jean F (2007) Grazing-induced changes in cell wall silicification in a marine diatom. *Protist* **158**, 21–28.
- Racki G, Cordey F (2000) Radiolarian paleoecology and radiolarites: is the present the key to the past? *Earth Science Reviews* **52**, 83–120.
- Ragueneau O, Treguer P, Leynaert A, Andersen RF, Brzezinski MA, DeMaster DJ, Dugdale RC, Dymond J, Fischer G, Francois R (2000) A review of the Si cycle in the modern ocean: recent progress and missing gaps in the application of biogenic opal as a paleo-productivity proxy. *Global and Planetary Change* **26**, 317–365.
- Raven JA, Waite AM (2004) The evolution of silicification in diatoms: inescapable sinking and sinking as escape? *New Phytologist* **162**, 45–61.
- Round FE, Crawford RM, Mann DG (1990) *The Diatoms: Biology and Morphology of the Genera*. Cambridge University Press, Cambridge.

- Sarmiento JL, Gruber N (2006) *Ocean Biogeochemical Dynamics*. Princeton University Press, Princeton, NJ.
- Siever R (1991) Silica in the oceans: biological-geochemical interplay. In *Scientists on Gaia* (eds Schneider SH, Boston PJ). The MIT Press, Boston, MA. pp. 287–295.
- Smetacek VS (1985) Role of sinking in diatom life-history cycles: ecological, evolutionary and geological significance. *Marine Biology* **84**, 239–251.
- Sommer U (1998) Silicate and the functional geometry of marine phytoplankton. *Journal of Plankton Research* **20**, 1853–1859.
- Strickland JDH, Parsons TR (1972) *A Practical Handbook of Seawater Analysis: Bulletin Fisheries Research Board of Canada*, Vol. **167**. Government of Canada, Ottawa, p. 311.
- Thamtrakoln K, Alverson AJ, Hildebrand M (2006) Comparative sequence analysis of diatom silicon transporters: towards a mechanistic model of silicon transport. *Journal of Phycology* **42**, 822–834.
- Thomsen K (2004) *Approximate Surface Area of a Scalene Ellipsoid*. Available at: Numerica.com.
- Tiffany MA, Hernández-Becerril DU (2005) Valve development in the diatom family Asterolampraceae H.L. Smith 1872. *Micropaleontology* **51**, 1–27.
- Tréguer P, Nelson D, Vanbennekom A, DeMaster D, Leynaert A, Queguiner B (1995) The silica balance in the world ocean – a reestimate. *Science* **268**, 375–379.
- Ukeles R (1973) Continuous culture – a method for the production of unicellular algal foods. In *Handbook of Phycological Methods: Culture Methods and Growth Measurements* (ed. Stein JL). Cambridge University Press, Cambridge, pp. 233–254.
- Williams DM, Round FE (1987) Revision of the genus *Fragilaria*. *Diatom Research* **2**, 267–288.
- Wischmeyer AG, Del Amo Y, Brzezinski M, Wolf-Gladrow DA (2003) Theoretical constraints on the uptake of silicic acid species by marine diatoms. *Marine Chemistry* **82**, 13–29.